



# Effects of diet and hyperlipidemia on levels and distribution of circulating lysophosphatidic acid

Maria P. Kraemer,<sup>\*,†</sup> Guogen Mao,<sup>\*,†</sup> Courtney Hammill,<sup>\*,†</sup> Baoxiang Yan,<sup>\*</sup> Yu Li,<sup>\*</sup> Fredrick Onono,<sup>\*</sup> Susan S. Smyth,<sup>\*,†</sup> and Andrew J. Morris<sup>1,\*,†</sup>

Division of Cardiovascular Medicine,<sup>\*</sup> Gill Heart and Vascular Institute, University of Kentucky, Lexington, KY; and Lexington Veterans Affairs Medical Center,<sup>†</sup> Lexington, KY

ORCID IDs: 0000-0003-3827-5045 (F.O.); 0000-0003-1910-4865 (A.J.M.)

**Abstract** Lysophosphatidic acids (LPAs) are bioactive radyl hydrocarbon-substituted derivatives of glycerol 3-phosphate. LPA metabolism and signaling are implicated in heritable risk of coronary artery disease. Genetic and pharmacological inhibition of these processes attenuate experimental atherosclerosis. LPA accumulates in atheromas, which may be a consequence of association with LDLs. The source, regulation, and biological activity of LDL-associated LPA are unknown. We examined the effects of experimental hyperlipidemia on the levels and distribution of circulating LPA in mice. The majority of plasma LPA was associated with albumin in plasma from wild-type mice fed normal chow. LDL-associated LPA was increased in plasma from high-fat Western diet-fed mice that are genetically prone to hyperlipidemia (LDL receptor knockout or activated proprotein convertase subtilisin/kexin type 9-overexpressing C57Bl6). Adipose-specific deficiency of the *ENPP2* gene encoding the LPA-generating secreted lysophospholipase D, autotaxin (ATX), attenuated these Western diet-dependent increases in LPA. ATX-dependent increases in LDL-associated LPA were observed in isolated incubated plasma. ATX acted directly on LDL-associated lysophospholipid substrates *in vitro*. LDL from all human subjects examined contained LPA and was decreased by lipid-lowering drug therapies. **Human and mouse plasma therefore contains a diet-sensitive LDL-associated LPA pool that might contribute to the cardiovascular disease-promoting effects of LPA.**—Kraemer, M. P., G. Mao, C. Hammill, B. Yan, Y. Li, F. Onono, S. S. Smyth, and Andrew J. Morris. **Effects of diet and hyperlipidemia on levels and distribution of circulating lysophosphatidic acid.** *J. Lipid Res.* 2019. 60: 1818–1828.

**Supplementary key words** cholesterol • lipoprotein • low density lipoprotein • autotaxin • mass spectrometry

Lysophosphatidic acids (LPAs) are a class of small receptor active phospholipid signaling molecules that promote the growth, survival, and motility of many cell types. LPA, its receptors and enzymes involved in LPA generation and inactivation are implicated in many pathologies including cardiovascular, pulmonary, and neurological diseases, and cancer (1–3). These observations underscore the importance of identifying the sources and mechanisms regulating the bioavailability and signaling actions of LPA that underlie this association with disease processes. LPA is abundant in plasma where it is primarily generated by hydrolysis of lysophospholipids [notably lysophosphatidylcholine (LPC)] by the secreted phospholipase, autotaxin (ATX) (4, 5), and can be degraded by phospholipases and lipid phosphatases, which may contribute to turnover of circulating LPA pools (3, 4). There is significant inter-individual variability in plasma LPA levels in humans (6). Despite some provocative observations, efforts to associate plasma LPA levels with human disease risk have largely been unsuccessful (7). Plasma LPA is prominently associated with serum albumin (6). Lysophospholipids are present in HDLs and LDLs (8); and LDL, particularly oxidized LDL, contains bioactive LPA (9, 10). This association of LPA with LDL is particularly relevant to the possible role of LPA in cardiovascular disease because of the central role played by LDL in atherosclerosis. However, at present, little is known about the metabolism and function of LDL-associated LPA.

Understanding the regulation of LPA metabolism and signaling in cardiovascular disease is important because, in humans, heritable variants of the *PLPP3* gene encoding lipid phosphate phosphatase 3 (LPP3), an enzyme that can

This work was supported by Department of Veterans Affairs Grants CX001550BX001984 and CX001550, National Heart, Lung, and Blood Institute Grant HL120507, and National Institute of General Medical Sciences Grant GM103527 to A.J.M. and S.S.S. F.O. is the recipient of National Institutes of Health, National Cancer Institute Mentored Research Scientist Development Award K01CA197073. M.P.K. was supported by a Postdoctoral Fellowship from the American Heart Association (18POST33960327). This research benefited from resources provided by the Lexington Veterans Affairs Medical Center. The content is solely the responsibility of the authors and does not necessarily represent the official views of the National Institutes of Health.

Manuscript received 8 February 2019 and in revised form 19 August 2019.

Published, JLR Papers in Press, September 4, 2019

DOI <https://doi.org/10.1194/jlr.M093096>

Abbreviations: ATX, autotaxin; LDLr, LDL receptor; LPA, lysophosphatidic acid; LPC, lysophosphatidylcholine; PCSK9, proprotein convertase subtilisin/kexin type 9.

<sup>1</sup>To whom correspondence should be addressed.

e-mail: [a.j.morris@uky.edu](mailto:a.j.morris@uky.edu)

dephosphorylate and inactivate LPA, are associated with inter-individual variability in coronary artery disease risk (11). The risk-associated variants disrupt regulatory elements that normally increase *PLPP3* expression, suggesting that attenuated inactivation of LPA signaling may underlie increased risk of coronary artery disease (12–14). LPA elicits cellular responses via activation of at least seven well-characterized G protein-coupled cell surface receptors (15). LPA receptors are expressed by platelets, vascular smooth muscle, and vascular endothelial cells (16). The atherosclerosis- and thrombosis-promoting actions of LPA are likely a result of LPA receptor-mediated effects on platelet activation, disruption of the endothelial cell barrier, monocyte attraction and adhesion, phenotypic modulation of vascular smooth muscle cells, and release of pro-inflammatory cytokines (10, 15, 17–23). LPA accumulates in human and experimentally induced mouse atheromas (9, 24, 25), and mice with genetic deficiency or pharmacological antagonism of certain LPA receptors are protected from atherosclerosis (10, 26).

High-fat diets exacerbate pathophysiological events that are associated with dysregulation of LPA metabolism and signaling. For example, in the LDL receptor-null (*Ldlr*<sup>-/-</sup>) mouse model of atherosclerosis, a high-fat atherosclerosis-promoting Western diet results in increased levels of ATX-derived LPA that promote inflammation and dyslipidemia (26). Furthermore, studies investigating adipose-specific knockout of the *ENPP2* gene encoding ATX reveal that adipose-derived ATX contributes to elevated circulating LPA levels in high-fat diet-fed mice (27, 28). Taken together, there is substantial evidence for a role of ATX-derived LPA in diet-induced hyperlipidemia and its complications, including atherosclerosis and diabetes (29).

To elucidate the relationship between diet and lipoprotein-associated LPA in mouse models of atherosclerosis, we measured the levels and molecular species profiles of LPA associated with different plasma lipoprotein pools and examined the role of ATX in regulating LDL-associated LPA. Our results demonstrate that a high-fat atherosclerosis-promoting diet in combination with genetically induced hyperlipidemia results in elevated LDL-associated LPA in mice, and that ATX can act directly on LDL-associated lysophospholipids to generate LPA. These observations appear translatable to humans because LPA was associated with LDL in plasma from all human subjects examined. In a subset of these subjects, lipid-lowering drug therapies decreased this pool of circulating LDL-associated LPA. These results identify a role for ATX in the generation of a diet-sensitive LDL-associated LPA pool and raise the possibility that LDL-associated LPA could play an important role in LPA-mediated cardiovascular disease processes.

## MATERIALS AND METHODS

### Mice

The Institutional Animal Care and Use Committee at the Lexington Veterans Affairs Medical Center approved all procedures. Trained veterinary staff and animal facility personnel monitored

the mice daily. Mice were housed in a temperature- and light-controlled facility (12 h light; 12 h dark) with water and food ad libitum. To investigate the effects of hyperlipidemia on plasma LPA distribution, plasma from mice with genetically induced hyperlipidemia fed the high-fat Western diet (see below) were compared with control mice hand fed a normal chow diet. Plasma samples were collected via submandibular bleed from wild-type C57Bl6, *LDLr*<sup>-/-</sup>, *ApoE*<sup>-/-</sup>, or C57Bl6 mice infected with recombinant adeno-associated viruses expressing the activated D377Y allele of PCSK9 either before or after feeding normal chow or a matched high-fat-containing Western diet (Envigo Teklad; TD.88137) for 8 weeks. This is a calorie-adjusted diet in which 42% of the total calories come from fat. Critical features of the diet include 0.2% total cholesterol by weight, 21% total fat by weight (>60% saturated fatty acids), and high sucrose (34% by weight). Proprotein convertase subtilisin/kexin type 9 (PCSK9)-expressing adeno-associated viruses were administered by a 100  $\mu$ l ip injection of PCSK9D377Y.AAV (University of Pennsylvania Vector Core) containing a total of  $20 \times 10^{10}$  genomic copies. The contribution of adipose-derived ATX was assessed by analyzing plasma from *ENPP2* fl/fl mice expressing adiponectin promoter drive Cre recombinase (*Adipoq-Cre*) resulting in loss of ATX expression in adipocytes (*Adipoq- $\Delta$* ). These mice were infected with the activated PCSK9-expressing adeno-associated virus and fed the high-fat Western diet for 16 weeks (30). For blood collection, EDTA:CTAD (1:5) was used as an anticoagulant except when ATX activity was assessed, in which case heparin was used for collection.

### Human plasma

De-identified human plasma was obtained from subjects enrolled in an Institutional Review Board-approved protocol as part of an ongoing study at the University of Kentucky or were purchased as de-identified samples from BioIVT (Westbury, NY). For studies of the effect of lipid-lowering therapy, plasma samples were obtained from subjects prior to and >4 weeks after initiation of oral statin therapy (atorvastatin, 40 mg/day). Informed consent was obtained from these subjects and the study conformed to the principles detailed in the World Medical Association Declaration of Helsinki.

### Plasma fractionation

One hundred microliters of plasma from individual mice or obtained from human subjects were fractionated by size-exclusion chromatography using a calibrated Superose 6 increase 10/300GL column (GE Healthcare) attached to an Agilent 1100 HPLC system using methods adapted from (31). The column was equilibrated and eluted with PBS at a flow rate of 0.5 ml/min. The eluate was collected into a 96-deep-well plate using an Agilent 1200 (G1364B) fraction collector. We collected 24 fractions and the volume of each fraction was 497 microliters. The separations were validated using Western blotting with antibodies against appropriate apolipoproteins or serum albumin to identify fractions containing HDL, LDL, VLDL, or serum albumin. Mouse plasma fractions were analyzed for cholesterol or triglyceride content and processed for LPA measurements as detailed below.

### Precipitation of human LDL for LPA analysis

Standard laboratory test methods were used to precipitate LDL from human plasma to assay LPA associated with LDL (32). LPA content of LDL was analyzed in a cohort ( $n = 17$ ) of human plasma samples with a range of varying clinically reported LDL cholesterol levels. 50  $\mu$ l of precipitant [5 mM EDTA (pH 4.2), 1 g/l polyvinyl sulfate, 169 g/l polyethylene glycol methyl ether] was mixed with 100  $\mu$ l of plasma. The mixture was incubated at room temperature for 30 min and then centrifuged at 1,500 g for

15 min. Lipids were extracted from the VLDL- and LDL-containing precipitates and their LPA content determined as described below.

### Lipid extraction and LC-MS/MS measurements of LPA

Seventeen LPA species were measured using techniques adapted from previously published methods (33). Briefly, either 50  $\mu$ l of whole plasma or 250  $\mu$ l of each plasma fraction were extracted using acidified organic solvents; the organic phases were evaporated to dryness and reconstituted for analysis. Fifty picomoles of 17:0 LPA (Avanti Polar Lipids Inc., Alabaster, AL) were included in each sample as an internal standard. LPA was measured using a Shimadzu HPLC coupled with an AB Sciex 6500-QTRAP hybrid linear ion trap triple quadrupole mass spectrometer operated in multiple reaction monitoring (MRM) mode. Samples were separated on a ACQUITY UPLC BEH C8, 1.7  $\mu$ m, 2.1  $\times$  100 mm column with an ACQUITY UPLC BEH C8 VanGuard Precolumn, 1.7  $\mu$ m, 2.1  $\times$  5 mm. Precursor-product ion pairs used for quantitation were as follows: 381.2/152.9 for 14:0, 395.2/153.0 for 15:0, 409.2/153.0 for 16:0, 407.0/153.0 for 16:1, 423.2/153.0 for 17:0, 437.2/152.8 for 18:0, 435.2/153.0 for 18:1, 433.0/153.0 for 18:2, 431.0/153.0 for 18:3, 451.3/152.9 for 19:0, 463.03/153.0 for 20:0, 461.01/153.0 for 20:2, 459.1/153.0 for 20:3, 457.1/152.8 for 20:4, 455.1/153.0 for 20:5, 485.1/153.0 for 22:2, 483.1/153.0 for 22:4, and 481.1/153.0 for 22:6. Data were analyzed using ABSciex Multiquant software, and LPA concentrations (in picomoles) were determined using the internal standard as a reference.

### Cholesterol measurements

Total plasma cholesterol was determined using a colorimetric assay (Pointe Scientific; C7510). Fractionated plasma cholesterol was determined with a more sensitive fluorometric assay, Amplex Red cholesterol assay kit (Invitrogen; A12216).

### Human ATX $\beta$ cloning and recombinant protein expression and purification

The ATX $\beta$  cDNA was cloned from a human brain cDNA library. The full-length ATX $\beta$  sequence was PCR-amplified and ligated into a modified pFastBac-1 (Life Technologies, Carlsbad, CA) vector to append a C-terminal SNAP-6x His tag coding sequence. The resulting pFastBac-ATX $\beta$ -SNAP-6xHis construct was transformed into DH10Bac cells (Life Technologies), and bacmid DNA was isolated and used to transfect BTI-TN-5B1-4 (High Five<sup>TM</sup>) cells to generate recombinant baculovirus. The amplified baculovirus (P3) was used to express mature secreted ATX $\beta$ . Protein expression in Express Five<sup>TM</sup> SFM cells (Life Technologies) was analyzed by immunoblotting using rabbit anti-ATX polyclonal antibody. Conditioned Express Five<sup>TM</sup> SFM culture medium (~1,000 ml) was collected and clarified by centrifugation at 400 *g* for 30 min, and by filtration through a 0.45  $\mu$ m bottle-top filter. The conditioned medium was then concentrated using a Pellicon<sup>®</sup> XL device (PXB030A50, NMWL 30 kDa) and LabScale<sup>TM</sup> tangential flow filtration system to ~100 ml and either used immediately or stored frozen at  $-80^{\circ}\text{C}$ . The concentrated ATX $\beta$ -containing medium was loaded onto a GE HisTrap<sup>TM</sup> (Life Sciences, Pittsburgh, PA) FF 2  $\times$  5 ml tandem column and the column was washed with 10 column volumes of buffer A [25 mM HEPES-KOH (pH 8.0), 500 mM NaCl, 10% glycerol, and 10 mM imidazole]. The ATX $\beta$  protein was eluted with a linear gradient to buffer A containing 800 mM imidazole. The fractions containing ATX $\beta$  protein were pooled and dialyzed overnight at  $4^{\circ}\text{C}$  in buffer PBE150 [25 mM HEPES-KOH (pH 8.0), 150 mM NaCl, 1 mM DTT, 0.1 mM EDTA, and 10% glycerol]. BSA (1 mg/ml) was added and aliquots of ATX $\beta$  were flash-frozen in liquid nitrogen and stored at  $-80^{\circ}\text{C}$ . The purity of the recombinant ATX $\beta$  proteins was assessed by SDS-PAGE and by Western blot for anti-ATX

(polyclonal antibody; Cayman Chemical Co., Ann Arbor, MI; #10005375). Protein concentrations were determined by Bradford assay. The specific enzymatic activity of the recombinant protein was comparable to that reported by ourselves and others (34).

### In vitro measurement of ATX activity against LDL-associated substrates

Four hundred nanograms of isolated human LDL free of EDTA (Lee Biosolutions, Maryland Heights, MO; 360-10) were incubated at  $37^{\circ}\text{C}$  for 4 h with 2 ng/ $\mu$ l recombinant human ATX $\beta$  in assay buffer [100 mM Tris (pH 8.0), 400 mM NaCl, 5 mM MgCl<sub>2</sub>, 5 mM CaCl<sub>2</sub>, 10  $\mu$ M CoCl<sub>2</sub>] modified from (35) and samples processed for MS measurements of LPA. The ATX dependence of increases in LPA was determined by including a potent ATX inhibitor, 1  $\mu$ M PF-8380, in the incubations (Sigma-Aldrich, St. Louis, MO; SML0715). LPC (15:0; 1 mM) was used as an exogenous substrate to monitor activity of the recombinant human ATX $\beta$ , and activity was quantified by MS measurement of 15:0 LPA. In other experiments, endogenous ATX activity in mouse plasma was measured by incubating heparin-collected plasma from LDLr<sup>-/-</sup> mice fed the high-fat Western diet for 8 weeks at  $37^{\circ}\text{C}$  for 12 h and then fractionating the plasma by size-exclusion chromatography and quantifying LPA species associated with each fraction by MS. Albumin bound-LPA was prepared by preincubating fatty acid-free BSA (Sigma-Aldrich; A8806) with 17:0 LPA for 4 h at  $37^{\circ}\text{C}$ . This LPA-BSA complex was then incubated with or without isolated human LDL overnight. These incubated plasma preparations were then fractionated by size-exclusion chromatography to separate LDL from albumin; lipids were extracted from the fractions and 17:0 LPA quantified by MS.

### Statistical analysis

The statistical tests detailed in the Results section and figure legends were performed using Sigma Stat software (Systat Inc., San Jose, CA). Statistical significance parameters are reported in the figure legends and the text.

## RESULTS

### Adipose-derived ATX mediates diet-dependent increases in LDL-associated LPA in genetically hyperlipidemic mouse models

We assessed the effects of diet and genetically induced hyperlipidemia on circulating LPA by comparing plasma LPA levels from different hyperlipidemic mouse models. Total plasma cholesterol determined using colorimetric enzymatic assays and plasma LPA measured using MS methods were compared between wild-type and genetically hyperlipidemic mice fed control or lipid-rich Western diets. We fractionated plasma using standard size-elution chromatography methods to assess the levels of LPA associated with albumin, HDL, or LDL. In wild-type C57Bl6 mice fed a Western diet for 8 weeks, total cholesterol increased slightly primarily due to a rise in HDL-associated cholesterol (Fig. 1A, B). High-fat Western diet-fed wild-type mice exhibited an increase in total plasma LPA because of significantly increased HDL-associated LPA (Fig. 2A, D). In mice that are genetically hyperlipidemic (Ldlr<sup>-/-</sup> mice or mice overexpressing activated PCSK9, which is a protease that inactivates the LDLr) and whose plasma cholesterol was substantially higher due to elevated LDL-associated cholesterol (Fig. 1A-C), total plasma LPA was also elevated.



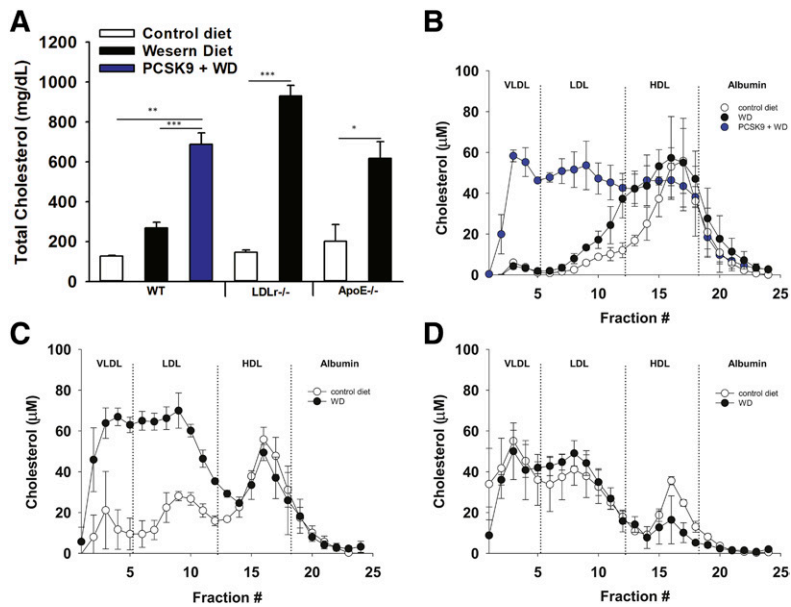


**Fig. 1.** Levels and distribution of cholesterol in plasma from mouse models used in this study. A: Total plasma cholesterol from wild-type mice, wild-type mice overexpressing activated PCSK9,  $LDLr^{-/-}$ , and  $ApoE^{-/-}$  mice on control chow or Western diet (WD) for 8 weeks. Quantification of cholesterol in 100  $\mu$ l of plasma fractionated by size-exclusion chromatography comparing lipoprotein-associated levels of cholesterol from the indicated treatment groups of wild-type mice (B),  $LDLr^{-/-}$  mice (C), and  $ApoE^{-/-}$  mice (D). Fractions associated with different lipoprotein pools are indicated by dotted lines and labels at the top of each graph ( $n = 3$ ). \* $P < 0.05$ , \*\* $P < 0.001$ , \*\*\* $P < 0.0001$  determined by Student's  $t$ -test.

This increase was due to significantly higher VLDL-, LDL-, and HDL-associated LPA (Fig. 2A–D).  $ApoE^{-/-}$  mice exhibited only significantly elevated VLDL-associated LPA (Fig. 2B), which is distinct from the increases in LPA associated with other lipoprotein pools observed in LDL-driven hyperlipidemic models ( $LDLr^{-/-}$  and activated PCSK9-overexpressing mice). There were no significant diet-dependent differences in the amount of LPA associated with albumin between any of the experimental groups of mice (Fig. 2E). For reasons that we do not fully understand, as

is apparent from Figs. 1 and 2 and **Table 1**, there is significant inter-individual variability in plasma LPA levels between mice with the same genotype fed the same diets. Despite this variability, our observation that the high-fat-containing Western diet significantly increased LDL-associated LPA was consistent in two completely independent studies (Table 1).

Because atherogenic LDL and VLDL play an important role in the development and progression of atherosclerosis, we focused on understanding the basis for our observation that LDL-associated LPA is increased in mice fed the

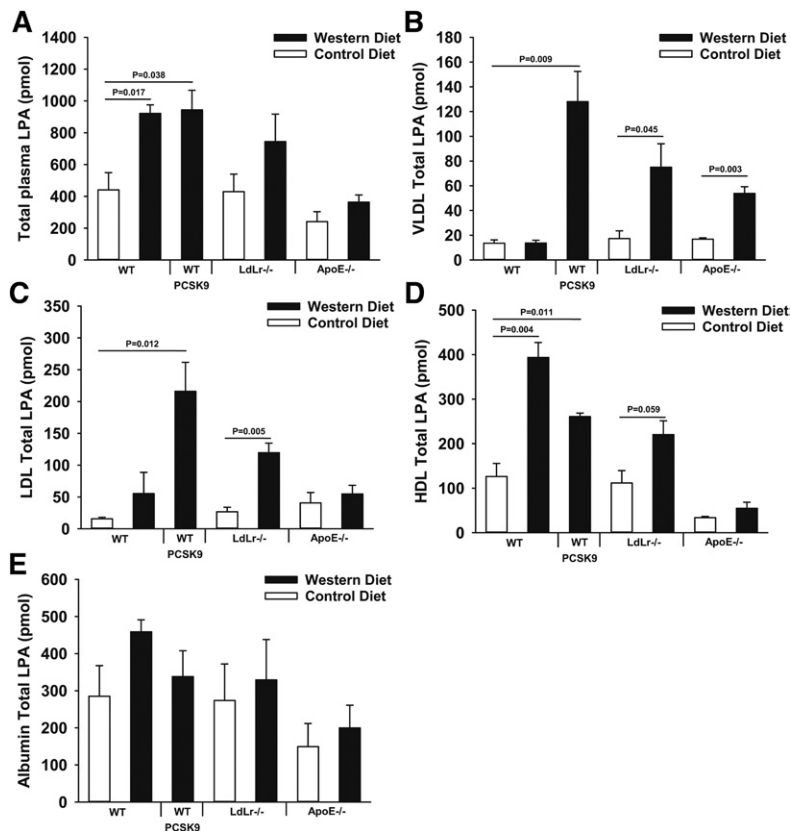


**Fig. 2.** Diet-dependent differences in levels and distribution of plasma LPA in wild-type, activated PCSK9-overexpressing,  $LDLr^{-/-}$ , and  $ApoE^{-/-}$  mice. Measurements of LPA from whole plasma (A) or 100  $\mu$ l of plasma fractionated by size-exclusion chromatography. Fractionated plasma results are presented as total amounts of LPA associated with VLDL (B), LDL (C), HDL (D), or albumin (E). LPA measurements represent the sum of all LPA species detected ( $n = 3$ ).  $P$  values were determined by Student's  $t$ -test.

TABLE 1. LDL-LPA increases in high-fat Western diet-fed mice

	Experiment 1 (n = 3)		Experiment 2 (n = 3)	
	Control Diet	Western Diet	Control Diet	Western Diet
Wild-type				
Total LPA	440.64 ± 108.46	921.70 ± 54.09	369.28 ± 6.59	378.72 ± 26.48
LDL-LPA	15.64 ± 2.38	55.31 ± 33.29	7.27 ± 0.22	7.45 ± 0.90
Fold increase		3.54		1.02
ApoE <sup>-/-</sup>				
Total LPA	240.58 ± 108.92	363.31 ± 78.67	467.37 ± 32.21	444.20 ± 43.02
LDL-LPA	57.37 ± 28.80	108.55 ± 31.52	9.20 ± 0.63	138.39 ± 13.40 <sup>a</sup>
Fold increase		1.89		15.40
LDLr <sup>-/-</sup>				
Total LPA	429.47 ± 110.00	744.19 ± 173.37	530.41 ± 77.31	514.53 ± 186.14
LDL-LPA	26.61 ± 7.19	119.59 ± 15.07 <sup>a</sup>	11.09 ± 1.69	322.15 ± 53.93 <sup>a</sup>
Fold increase		4.49		29.00

Summary of two independent mouse studies quantifying LPA associated with LDL in mice of the indicated genotypes fed control or high-fat Western diets. Values are reported as mean ± SEM (n = 3). Experiment 1 represents the data presented in detail in Figs. 2 and 3.

<sup>a</sup>Comparisons between LPA in the indicated fractions obtained from mice fed the control or Western diet were assessed by unpaired Student's *t*-test, *P* < 0.05.

high-fat Western diet when LDL levels are elevated by LDLr deficiency or overexpression of activated PCSK9. Interestingly, when activated PCSK9-overexpressing wild-type mice or LDLr<sup>-/-</sup> mice become hyperlipidemic after feeding the Western diet, particular LPA species were detected in LDL. We observed significant increases in 16:0, 18:0, 18:1, 18:2, 19:0, 20:0, 20:2, 20:3, 20:4, and 22:4 LPA, with the most prominent species observed being 18:0, 16:0, 18:1, and 22:6 (Fig. 3). We found that this rise in LPA spe-

cies is largely mediated by adipose-derived ATX because mice that have reduced ATX expression in adipocytes (Adipoq-Δ) (30) did not exhibit elevated VLDL- and LDL-associated LPA even after being fed the Western diet for 16 weeks post PCSK9 adeno-associated virus infection (Fig. 4). Note that LDL and VLDL cholesterol levels in these ATX-deficient mice were not different from wild-type controls. Adipoq-Δ mice exhibit protection against hepatic steatosis that develops in response to high-fat feeding

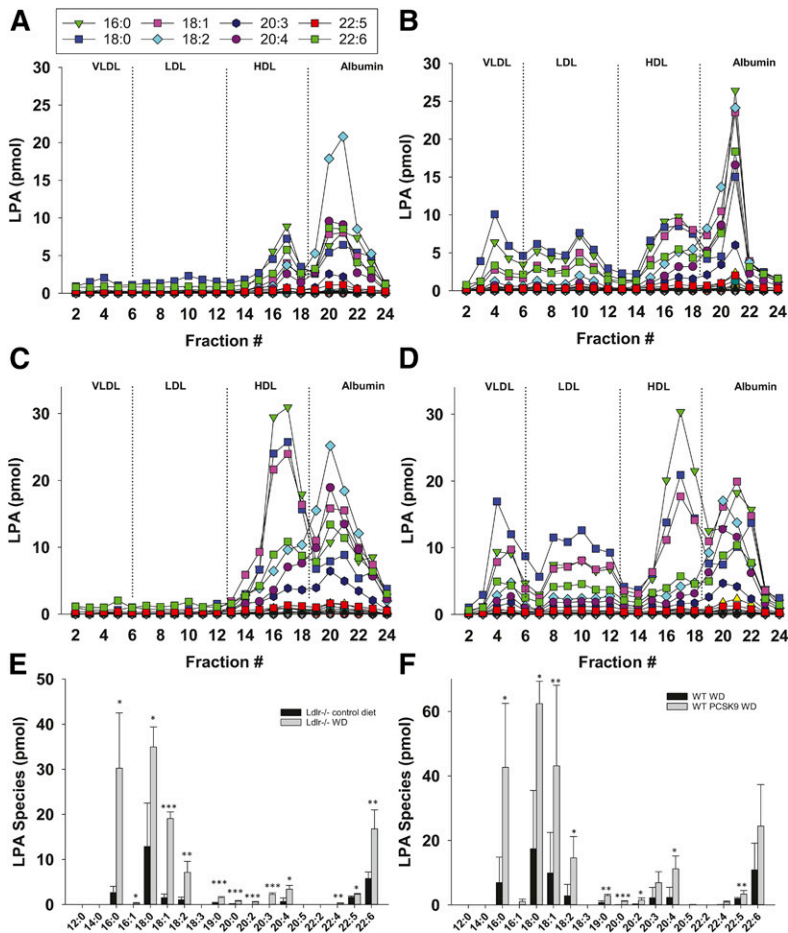
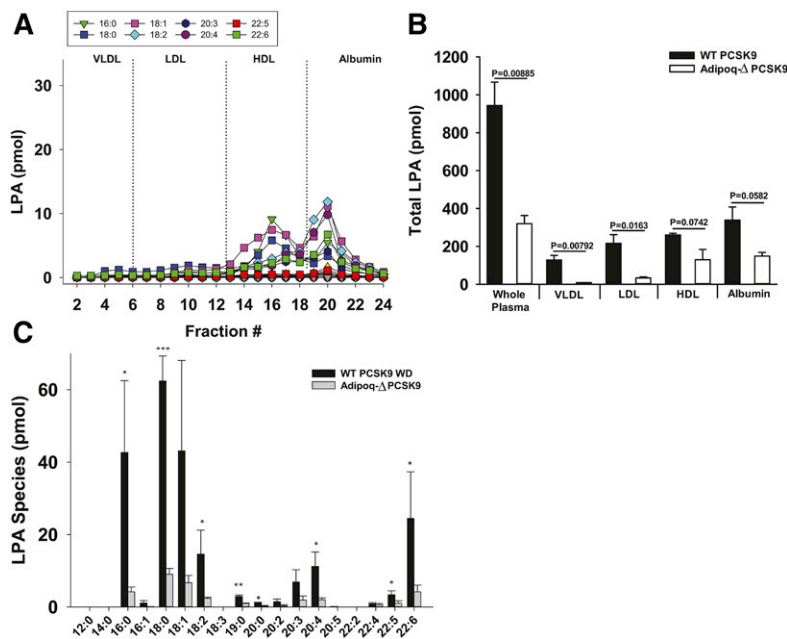


Fig. 3. Specific LPA species are elevated in LDL of hyperlipidemic mice. Representative data showing the levels of the indicated LPA species present in each fraction from FPLC-fractionated plasma (100 μl) from an LDLr<sup>-/-</sup> mouse fed control diet (A) or high-fat Western diet (B). Representative data showing levels of the indicated LPA species in fractionated plasma from a wild-type mouse fed Western diet (C) or from an activated PCSK9-overexpressing mouse fed Western diet (D). E: Comparison of individual LPA species in the LDL-containing fractions from LDLr<sup>-/-</sup> mice (fractions 6–13) fed either the control or the high-fat Western diet (n = 3). F: Comparison of individual LPA species in the LDL-associated fractions isolated from plasma of wild-type mice or activated PCSK9-overexpressing mice fed the control or high-fat Western diet (n = 3). \**P* < 0.05, \*\**P* < 0.001, \*\*\**P* < 0.0001 determined by Student's *t*-test.



**Fig. 4.** Diet-dependent increases in plasma LPA require adipose-derived ATX. **A:** Representative data showing levels of the indicated LPA species present in fractionated plasma from a high-fat Western diet-fed activated PCSK9-overexpressing Adipoq- $\Delta$  mouse. **B:** Sum of all LPA species present in the indicated plasma lipoprotein pools isolated from activated PCSK9-overexpressing high-fat Western diet-fed Adipoq- $\Delta$  mice compared with lipoprotein-associated LPA levels determined in plasma from activated PCSK9-overexpressing Western diet-fed wild-type mice ( $n = 3$ ) (see also Fig. 3). **C:** Comparison of levels of the indicated LPA species in plasma LDL isolated from high-fat Western diet-fed activated PCSK9-overexpressing wild-type mice or from Western diet-fed activated PCSK9-overexpressing Adipoq- $\Delta$  mice- ( $n = 3$ ). \* $P < 0.05$ , \*\* $P < 0.001$ , \*\*\* $P < 0.0001$  determined by Student's  $t$ -test.

but are otherwise phenotypically unremarkable (30). LPA was detected in HDL and albumin fractions from Adipoq- $\Delta$  mice, although at lower levels than observed in wild-type mice expressing activated PCSK9, but these differences did not quite reach statistical significance. Note that Fig. 4 presents data for PCSK9-overexpressing mice from Figs. 2 and 3 to enable a direct comparison with data from PCSK9-overexpressing Adipoq- $\Delta$  mice.

#### LPA is associated with LDL in human subjects and decreased by lipid-lowering therapy

We were interested in determining whether our findings in mice would have relevance to humans. We analyzed human plasma from individuals with varying plasma cholesterol levels to determine whether LPA could be detected in LDL. We correlated LDL-LPA with clinically reported cholesterol values (Fig. 5A, B). Although not statistically significant by conventional criteria, both total plasma cholesterol and LDL-associated cholesterol showed a trend toward association with total plasma LPA and LDL-associated LPA. Most importantly, LDL isolated from all 17 subjects analyzed contained readily detectable levels of LPA. In light of this association between LDL and LPA, we wanted to determine whether LDL-associated LPA would be sensitive to lipid-lowering therapy. We assessed three subjects pre- and post-statin treatment (Fig. 5C–E, Table 2). Plasma samples obtained from subjects before and after initiation of statin therapy were separated by size-exclusion chromatography to enable analysis of the LPA content of different lipoprotein fractions. LPA was detected in LDL from each individual prior to initiation of lipid-lowering therapy (Table 2, Fig. 5C); however, this LPA pool was reduced in all subjects after initiation of lipid-lowering therapy (Table 2, Fig. 5C). Lipid fractionation profiles are shown for one subject. This individual had high plasma cholesterol (201 mg/dl) and exhibited significant LDL-associated LPA in the pretreatment sample (Fig. 5B). We

measured a loss of LDL-LPA in a second plasma sample (123 mg/dl total plasma cholesterol) from the same individual after initiation of therapy with atorvastatin (40 mg/day) (Fig. 5C).

#### ATX can generate LDL-associated LPA by direct hydrolysis of LDL-associated substrates

Increases in LDL-associated LPA were dependent on adipose-derived ATX in mice. To determine whether this might result from ATX-catalyzed direct hydrolysis of LDL-associated lysophospholipid substrates, we generated purified recombinant ATX $\beta$  and demonstrated that this preparation had robust enzymatic activity with the exogenous ATX substrate, 15:0 LPC, under the assay conditions used to examine activity against LDL-associated substrates (Fig. 6A, B). After incubating recombinant ATX $\beta$  with isolated human LDL for 4 h at 37°C in the absence of any other substrates, LPA was increased  $\sim 4$ -fold (Fig. 6C). The potent specific ATX inhibitor, PF-8380 (Fig. 6C), completely inhibited this increase in LDL-derived LPA. It is well-established that incubating plasma at 37°C results in substantial ATX-dependent increases in total plasma LPA (4). To test the possibility that ATX in plasma can act directly on LDL-associated substrates, we incubated plasma from high-fat Western diet-fed LDLr<sup>-/-</sup> mice overnight at 37°C and then fractionated the incubated plasma to examine potential increases in different lipoprotein-associated LPA pools. Incubation of plasma at 37°C resulted in increases in the LPA content of all of the lipoprotein fractions examined, including LDL, suggesting that endogenous ATX can directly act on LDL-associated substrates in plasma. Incubation of plasma at 37°C also resulted in a robust increase in serum albumin-associated LPA. We were therefore interested in examining the possibility that serum albumin-associated LPA could transfer to LDL in plasma. We therefore incubated BSA complexed with 17:0 LPA with isolated LDL, fractionated the mixture by size exclusion

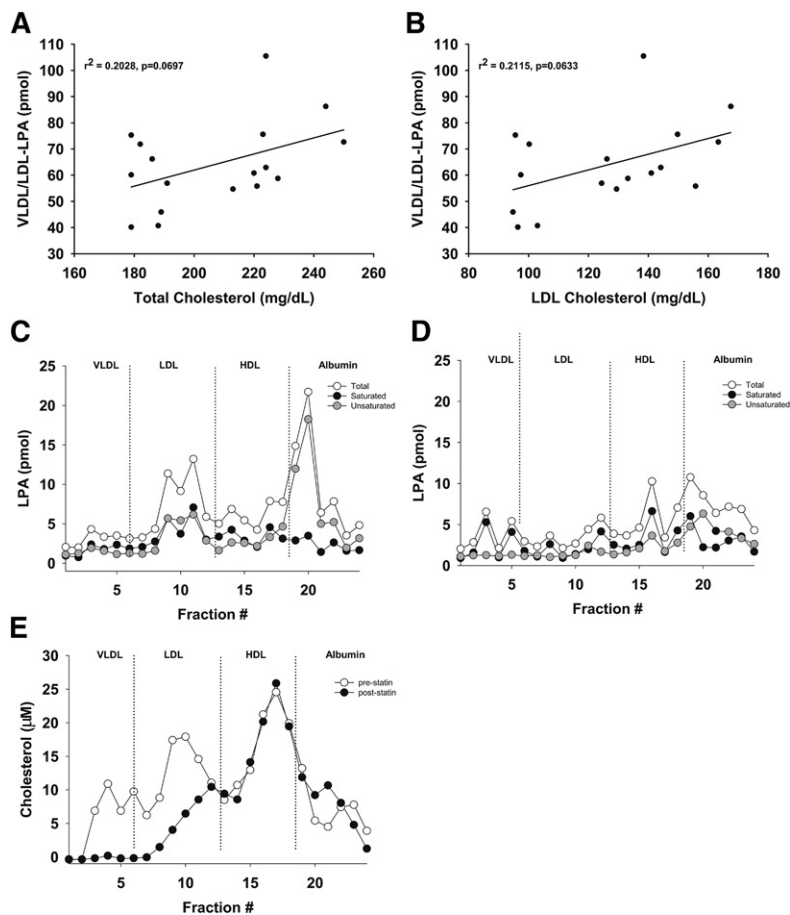


**Fig. 5.** LPA is associated with LDL from multiple human subjects and decreased by lipid-lowering drug therapy. **A:** Correlation between LPA associated with LDL isolated from human plasma and total plasma cholesterol. **B:** Correlation between LPA associated with LDL isolated from human plasma and LDL-associated cholesterol. In both cases, data ( $n = 17$ ) were analyzed by linear regression with  $r^2$  and  $P$  values reported in the figure. Representative data showing LPA levels from fractionated plasma collected prior to (**C**) or following (**D**) treatment with a statin. ( $n = 1$ ) (see also Table 2). **E:** Measurement of cholesterol from fractionated human plasma collected prior to and after treatment with a statin (atorvastatin, 40 mg/day).

chromatography, and then measured LDL-associated 17:0 LPA. In these experiments, we complexed 17:0 LPA with BSA at a molar ratio of 5:1 and incubated this with purified LDL at a final concentration of 0.1 mg/ml. After a 12 h

incubation, only  $0.68 \pm 0.01\%$  of the 17:0 LPA was associated with LDL. The most parsimonious interpretation of these data is that, while transfer of LPA from serum albumin to LDL can occur in vitro, this is unlikely to account for the more rapid and substantial ATX-dependent increases in LDL-associated LPA we observed in incubated plasma.

TABLE 2. Lipid-lowering statin therapy decreases LDL-associated LPA

	Patient 1	Patient 2	Patient 3
Total plasma cholesterol ( $\mu\text{M}$ )			
Pre-	249.86	47.50	79.82
Post-	173.13	33.81	10.05
Percent reduced	30.71%	28.82%	87.41%
LDL cholesterol ( $\mu\text{M}$ )			
Pre-	84.50	20.06	33.93
Post-	40.30	9.09	0.89
Percent reduced	52.3%	54.69%	97.39%
VLDL/LDL-LPA (all species, pmol)			
Pre-	65.54	60.42	16.44
Post-	42.93	15.33	8.35
Percent reduced	34.49%	74.63%	49.2%
HDL/albumin-LPA (all species, pmol)			
Pre-	91.31	71.30	87.09
Post-	73.10	57.95	16.27
Percent reduced	19.94%	18.72%	81.32%
Total-LPA (all species, pmol)			
Pre-	161.86	90.79	110.93
Post-	119.91	75.16	27.38
Percent reduced	25.91%	17.21%	75.32%

Measurements of LPA were made in whole plasma or isolated lipoprotein fractions from three individuals before (Pre-) and after (Post-) initiation of lipid-lowering statin drug therapy. One hundred microliters of plasma were fractionated and LPA levels in plasma or the individual lipoprotein fractions are normalized to this value.

## DISCUSSION

Common variants that determine expression levels of the PLPP3 gene encoding an enzyme that can degrade and inactivate LPA are associated with heritable cardiovascular disease risk in humans (13). This finding has prompted ongoing efforts to investigate LPA as a relevant pathophysiological mediator of cardiovascular disease and raise the possibility that circulating LPA could be a biomarker of cardiovascular disease risk. We report that diet can alter the levels of LPA associated with circulating lipoproteins in mice, and that a high-fat atherosclerosis-promoting diet in combination with genetic impairment of LDL clearance can substantially elevate LDL-associated LPA in plasma. We found that adipose-derived ATX is required for these dietary alterations of plasma LPA. Furthermore, we show that ATX can act directly on LDL-associated lysophospholipid substrates. These findings imply that adipose-derived ATX may directly alter LPA content of circulating LDL and demonstrate that diet has a marked impact on the plasma



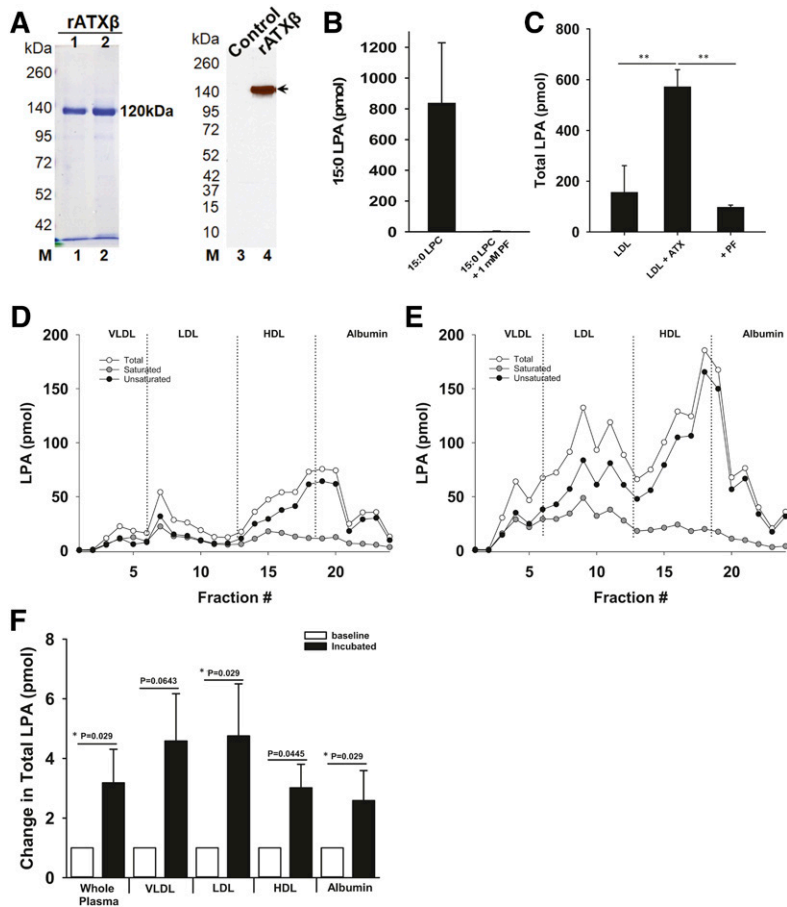


**Fig. 6.** ATX directly acts on LDL-associated substrates. **A:** Coomassie blue-stained gel and Western blot analysis of recombinant ATXβ protein preparations used in these experiments. **B:** Measurement of recombinant ATXβ activity using 15:0 LPC as a substrate under the assay conditions used for studies with LDL (n = 3). **C:** Measurement of ATX activity against isolated LDL-associated substrates determined in the presence or absence of the ATX inhibitor (1 μM), PF-8380 (n = 3–6). **D:** Data from a representative fractionation experiment showing the distribution of LPA present in plasma from a high-fat Western diet-fed LDL<sup>-/-</sup> mouse prior to (D) or following (E) an overnight incubation at 37°C. **F:** Summarized data from multiple experiments showing the increase in total LPA in whole mouse plasma or plasma lipoprotein fractions after overnight incubation at 37°C. P values indicate results of Student's *t*-test. \**P* indicates Mann-Whitney test. \**P* < 0.05, \*\**P* < 0.001, \*\*\**P* < 0.0001 determined by Student's *t*-test.

distribution of LPA that may in turn affect LPA-mediated signaling and associated disease risk.

Increases in plasma LPA have been associated with experimentally induced obesity and metabolic disease animal models, suggesting that plasma LPA could be a useful biomarker of these conditions in humans (36, 37). Several studies have attempted to identify particular LPA species that positively correlate with the prognosis of different diseases, such as obesity, asthma, and cancer (36, 38, 39). However, in these studies, despite efforts to prevent post collection increases in plasma LPA and the use of accurate and precise MS-based methods for measurement of LPA, inter-individual variability in total circulating LPA levels is substantial. This variability has hampered efforts to establish the usefulness of plasma LPA as a disease biomarker. Despite these challenges, recent studies have identified plasma 16:0 LPA as being elevated independently of other LPA species in obese rhesus monkeys (36). In humans, plasma 22:6 LPA, 18:2 LPA, and 20:4 LPA were found to be elevated in patients with acute coronary syndrome (40). Although the relationship with circulating LPA remains to be established, LPA is present in the lipid-rich core of human atherosclerotic plaques, with 16:0, 18:0, 18:1, and 20:4 being the most predominant species detected (24, 41, 42). In our mouse studies, we found that mouse and human LDL contain many of the LPA species reported to be increased in the plasma of obese humans and that accumulate in atherosclerotic lesions (Fig. 3E,

F). In particular, we found that 16:0, 18:0, 18:1, 18:2, and 22:6 were the most abundant LDL-associated LPA species. Our data support the idea that these LPA species might contribute to disease risk associated with elevated circulating LDL levels.

Obesity, atherosclerosis, and myocardial infarction have been reported to be associated with elevated circulating LPA levels (24, 37, 43). Diets that elevate levels of ApoB-containing LDLs accelerate the progression of atherosclerosis (44). Total plasma LPA is sensitive to manipulations of diet in mouse models and has been reported to positively correlate with cholesterol and body mass index in humans (6, 27). The mechanisms responsible for these apparent associations between plasma LPA levels and diet in humans are still unclear. Our results clearly demonstrate that levels and distribution of LPA in plasma are strongly influenced by high-fat diet feeding in mouse models. This acute sensitivity to diet could contribute to inter-individual variability in plasma LPA levels in humans. Furthermore, we found that in mice these diet-dependent changes in LDL-associated LPA required adipose-derived ATX (Fig. 4). The substantial decreases in LDL-associated LPA in ATX knockout mice (Fig. 4) might contribute to the improved glucose and insulin homeostasis observed by others in adipose-specific ATX knockout mice (45, 46).

Our observations of LDL-associated LPA in mice appear translatable to humans because LPA was present in LDL



from all subjects examined. Interestingly, our analysis of human plasma collected prior to and following initiation of lipid-lowering statin therapy support the concept that lipid lowering decreases this LDL-associated LPA pool. More extensive studies investigating changes in LPA plasma profiles caused by altered plasma lipids or diet are needed to make conclusions about how these physiological factors affect lipoprotein-associated LPA in humans and whether particular LPA species or specific pools of LPA correlate with cardiovascular health. Such studies would greatly enhance our understanding of the potential of plasma LPA or, more specifically, lipoprotein-associated LPA as a link between hyperlipidemia and cardiovascular disease.

We and others have shown that LPA is mainly associated with serum albumin in plasma from wild-type mice fed a normal diet (Figs. 1, 2) (47, 48). Although *in vitro* studies clearly show that albumin-bound LPA is biologically active, very little is known about how the signaling functions of LPA could be altered by association with lipoproteins and extracellular lipid vesicles (48). Recent reports indicate that ATX can act on HDL and exosome-associated substrates to generate LPA (49–51). Our present findings suggest that in the absence of genetically induced hyperlipidemia, a high-fat Western diet increases the abundance of LPA in HDL without raising levels of albumin-associated LPA (Figs. 1, 2). However, our fractionation method does not completely resolve HDL and serum albumin, so more definitive information about the effects of diet on HDL-associated LPA will require further studies. This is an important issue because HDL-associated LPA has been suggested to play a role in aortic valve calcification associated with obesity (50, 51).

Other groups have reported that LPA associates with oxidized-LDL and that the cellular effects of oxidized-LDL, such as increased monocyte adhesion to endothelial cells and platelet activation, require LPA signaling (9, 10). In the genetically hyperlipidemic models studied here, LDL-associated LPA accounted for as much as ~40% of the observed elevation in total plasma LPA elicited by feeding a high-fat Western diet, suggesting that under these conditions LDL-associated LPA could be biologically relevant. Our data also indicate that LDL-associated lysophospholipids can serve as direct substrates for ATX. LPC constitutes only 1–5% of the total phosphatidylcholine associated with LDL, but this is increased substantially by oxidation under which conditions 40–50% of LDL-associated phosphatidylcholine can be converted to LPC (52). Oxidation might therefore result in increased ATX-catalyzed generation of LDL-associated LPA because of this increase in substrate availability. Additional studies to determine whether LDL or oxidized-LDL containing higher levels of LPA has distinct signaling properties would provide insight into the potential contribution of LDL-associated LPA in mediating many of the pathological mechanisms linked to atherogenic LDL signaling. We also found that serum albumin-complexed LPA can transfer to LDL, albeit at a slow rate that was unlikely to account for the ATX-dependent increases in

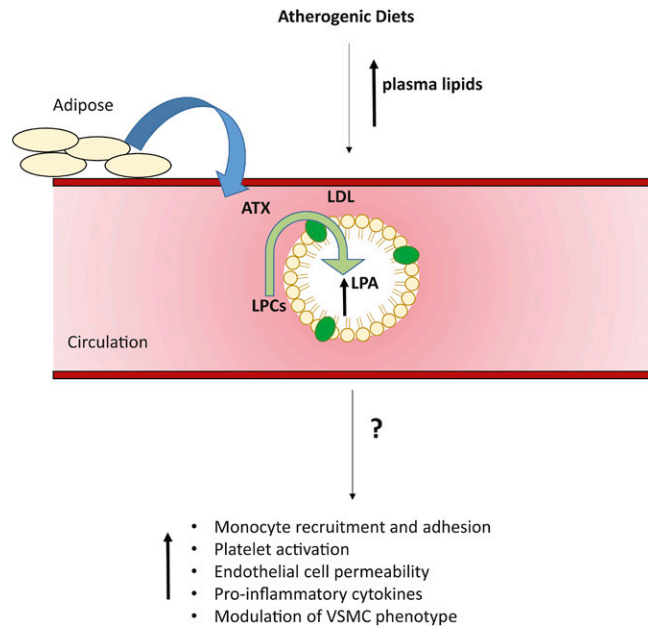


**Fig. 7.** Relationship between diet and circulating LDL-associated LPA. The figure summarizes our findings showing the possible link between high-fat atherosclerosis-promoting diets and circulating LPA. ATX, derived from adipose tissue, catalyzes the conversion of lysophospholipids to LPA in plasma. Increased levels of plasma LPA are observed in mice fed high-fat atherosclerosis-promoting diets. ATX can act directly on LDL-associated substrates to increase LDL-associated LPA. The possible impact of LPA on the pro-inflammatory and atherogenic actions of LDL remain to be established, but our findings suggest that LDL-associated LPA could be a link between diet and cell signaling events associated with increased cardiovascular disease risk.

LDL-associated LPA we observed in incubated plasma. Circulating LDL in humans is estimated to have a half-life of ~3 days based on measurements of ApoB, and, while turnover of LDL-associated cholesterol and triglycerides may be somewhat faster, nothing is known about turnover of less abundant LDL-associated lipids (53). More work is needed to assess the physiological importance of transfer of LPA between serum albumin and LDL.

In summary, we show that ATX can act on lipoprotein-associated lipid substrates and that diet and genetic manipulations that elevate LDL are associated with significant increases in LDL-associated LPA pools in mice. LPA is also associated with LDL isolated from multiple human subjects. These findings have important implications for efforts to identify associations between circulating LPA levels and human disease risk because they suggest that diet and levels of circulating lipoprotein, particularly LDL, are important determinants of plasma LPA levels. They also raise the possibility that, as has been demonstrated for other bioactive lipid mediators, association with lipoproteins (54) might “chaperone” the signaling actions of LPA to generate cell type-specific signaling responses that could be an important determinant of LPA signaling in cardiovascular disease processes (Fig. 7). Further work will be needed to explore these possibilities.

## REFERENCES

- Hisano, Y., and T. Hla. 2019. Bioactive lysolipids in cancer and angiogenesis. *Pharmacol. Ther.* **193**: 91–98.
- Herr, D. R., W. S. Chew, R. L. Satish, and W. Y. Ong. Pleotropic roles of autotaxin in the nervous system present opportunities for the development of novel therapeutics for neurological diseases. *Mol. Neurobiol.* Epub ahead of print. July 30, 2019; doi:10.1007/s12035-019-01719-1.
- Benesch, M. G. K., I. T. K. MacIntyre, T. P. W. McMullen, and D. N. Brindley. 2018. Coming of age for autotaxin and lysophosphatidate signaling: clinical applications for preventing, detecting and targeting tumor-promoting inflammation. *Cancers (Basel)*. **10**: E73.
- Aoki, J., A. Inoue, and S. Okudaira. 2008. Two pathways for lysophosphatidic acid production. *Biochim. Biophys. Acta*. **1781**: 513–518.
- Aoki, J., A. Taira, Y. Takanezawa, Y. Kishi, K. Hama, T. Kishimoto, K. Mizuno, K. Saku, R. Taguchi, and H. Arai. 2002. Serum lysophosphatidic acid is produced through diverse phospholipase pathways. *J. Biol. Chem.* **277**: 48737–48744.
- Michalczyk, A., M. Budkowska, B. Dolegowska, D. Chlubek, and K. Safranow. 2017. Lysophosphatidic acid plasma concentrations in healthy subjects: circadian rhythm and associations with demographic, anthropometric and biochemical parameters. *Lipids Health Dis.* **16**: 140.
- Yagi, T., M. Shoaib, C. Kuschner, M. Nishikimi, L. B. Becker, A. T. Lee, and J. Kim. 2019. Challenges and inconsistencies in using lysophosphatidic acid as a biomarker for ovarian cancer. *Cancers (Basel)*. **11**: E520.
- Rauschert, S., A. Gazquez, O. Uhl, F. F. Kirchberg, H. Demmelmair, M. Ruiz-Palacios, M. T. Prieto-Sanchez, J. E. Blanco-Carnero, A. Nieto, E. Larque, et al. 2019. Phospholipids in lipoproteins: compositional differences across VLDL, LDL, and HDL in pregnant women. *Lipids Health Dis.* **18**: 20.
- Siess, W., K. J. Zangl, M. Essler, M. Bauer, R. Brandl, C. Corrinth, R. Bittman, G. Tigyi, and M. Aepfelbacher. 1999. Lysophosphatidic acid mediates the rapid activation of platelets and endothelial cells by mildly oxidized low density lipoprotein and accumulates in human atherosclerotic lesions. *Proc. Natl. Acad. Sci. USA*. **96**: 6931–6936.
- Zhou, Z., P. Subramanian, G. Sevilimis, B. Globke, O. Soehnlein, E. Karshovska, R. Megens, K. Heyll, J. Chun, J. S. Saulnier-Blache, et al. 2011. Lipoprotein-derived lysophosphatidic acid promotes atherosclerosis by releasing CXCL1 from the endothelium. *Cell Metab.* **13**: 592–600.
- Busnelli, M., S. Manzini, C. Parolini, D. Escalante-Alcalde, and G. Chiesa. 2018. Lipid phosphate phosphatase 3 in vascular pathophysiology. *Atherosclerosis*. **271**: 156–165.
- Erbilgin, A., M. Civelek, C. E. Romanoski, C. Pan, R. Hagopian, J. A. Berliner, and A. J. Lusis. 2013. Identification of CAD candidate genes in GWAS loci and their expression in vascular cells. *J. Lipid Res.* **54**: 1894–1905.
- Reschen, M. E., K. J. Gaulton, D. Lin, E. J. Soilleux, A. J. Morris, S. S. Smyth, and C. A. O'Callaghan. 2015. Lipid-induced epigenomic changes in human macrophages identify a coronary artery disease-associated variant that regulates PPAP2B Expression through Altered C/EBP-beta binding. *PLoS Genet.* **11**: e1005061.
- Mao, G., S. S. Smyth, and A. J. Morris. Regulation of PLPP3 gene expression by NF-kB family transcription factors. *J. Biol. Chem.* Epub ahead of print. July 30, 2019; doi:10.1074/jbc.RA119.009002.
- Lin, M. E., D. R. Herr, and J. Chun. 2010. Lysophosphatidic acid (LPA) receptors: signaling properties and disease relevance. *Prostaglandins Other Lipid Mediat.* **91**: 130–138.
- Abdel-Latif, A., P. M. Heron, A. J. Morris, and S. S. Smyth. 2015. Lysophospholipids in coronary artery and chronic ischemic heart disease. *Curr. Opin. Lipidol.* **26**: 432–437.
- Hao, F., M. Tan, D. D. Wu, X. Xu, and M. Z. Cui. 2010. LPA induces IL-6 secretion from aortic smooth muscle cells via an LPA1-regulated, PKC-dependent, and p38alpha-mediated pathway. *Am. J. Physiol. Heart Circ. Physiol.* **298**: H974–H983.
- Siess, W., and G. Tigyi. 2004. Thrombogenic and atherogenic activities of lysophosphatidic acid. *J. Cell. Biochem.* **92**: 1086–1094.
- Mueller, P., S. Ye, A. Morris, and S. S. Smyth. 2015. Lysophospholipid mediators in the vasculature. *Exp. Cell Res.* **333**: 190–194.
- Galkina, E., and K. Ley. 2009. Immune and inflammatory mechanisms of atherosclerosis. *Annu. Rev. Immunol.* **27**: 165–197.
- Gibbs-Bar, L., H. Tempelhof, R. Ben-Hamo, Y. Ely, A. Brandis, R. Hofi, G. Almog, T. Braun, E. Feldmesser, S. Efroni, et al. 2016. Autotaxin-lysophosphatidic acid axis acts downstream of apolipoprotein B lipoproteins in endothelial cells. *Arterioscler. Thromb. Vasc. Biol.* **36**: 2058–2067.
- Kritikou, E., G. H. van Puijvelde, T. van der Heijden, P. J. van Santbrink, M. Swart, F. H. Schaftenaar, M. J. Kröner, J. Kuiper, and I. Bot. 2016. Inhibition of lysophosphatidic acid receptors 1 and 3 attenuates atherosclerosis development in LDL-receptor deficient mice. *Sci. Rep.* **6**: 37585.
- Smyth, S. S., P. Mueller, F. Yang, J. A. Brandon, and A. J. Morris. 2014. Arguing the case for the autotaxin-lysophosphatidic acid-lipid phosphate phosphatase 3-signaling nexus in the development and complications of atherosclerosis. *Arterioscler. Thromb. Vasc. Biol.* **34**: 479–486.
- Dohi, T., K. Miyauchi, R. Ohkawa, K. Nakamura, M. Kurano, T. Kishimoto, N. Yanagisawa, M. Ogita, T. Miyazaki, A. Nishino, et al. 2013. Increased lysophosphatidic acid levels in culprit coronary arteries of patients with acute coronary syndrome. *Atherosclerosis*. **229**: 192–197.
- Bot, M., S. C. de Jager, L. MacAleese, H. M. Lagraauw, T. J. van Berkel, P. H. Quax, J. Kuiper, R. M. Heeren, E. A. Biessen, and I. Bot. 2013. Lysophosphatidic acid triggers mast cell-driven atherosclerotic plaque destabilization by increasing vascular inflammation. *J. Lipid Res.* **54**: 1265–1274.
- Navab, M., G. Hough, G. M. Buga, F. Su, A. C. Wagner, D. Meriwether, A. Chattopadhyay, F. Gao, V. Grijalva, J. S. Danciger, et al. 2013. Transgenic 6F tomatoes act on the small intestine to prevent systemic inflammation and dyslipidemia caused by Western diet and intestinally derived lysophosphatidic acid. *J. Lipid Res.* **54**: 3403–3418.
- Dusauly, R., C. Rancoule, S. Gres, E. Wanecq, A. Colom, C. Guigne, L. A. van Meeteren, W. H. Moolenaar, P. Valet, and J. S. Saulnier-Blache. 2011. Adipose-specific disruption of autotaxin enhances nutritional fattening and reduces plasma lysophosphatidic acid. *J. Lipid Res.* **52**: 1247–1255.
- Federico, L., H. Ren, P. A. Mueller, T. Wu, S. Liu, J. Popovic, E. M. Blalock, M. Sunkara, H. Ova, H. M. Albers, et al. 2012. Autotaxin and its product lysophosphatidic acid suppress brown adipose differentiation and promote diet-induced obesity in mice. *Mol. Endocrinol.* **26**: 786–797.
- D'Souza, K., C. Nzirorera, A. M. Cowie, G. P. Varghese, P. Trivedi, T. O. Eichmann, D. Biswas, M. Touaibia, A. J. Morris, V. Aidinis, et al. 2018. Autotaxin-LPA signaling contributes to obesity-induced insulin resistance in muscle and impairs mitochondrial metabolism. *J. Lipid Res.* **59**: 1805–1817.
- Brandon, J. A., M. Kraemer, J. Vandra, S. Halder, M. Ubele, A. J. Morris, and S. S. Smyth. 2019. Adipose-derived autotaxin regulates inflammation and steatosis associated with diet-induced obesity. *PLoS One*. In press.
- Garber, D. W., K. R. Kulkarni, and G. M. Anantharamaiah. 2000. A sensitive and convenient method for lipoprotein profile analysis of individual mouse plasma samples. *J. Lipid Res.* **41**: 1020–1026.
- Kerscher, L., S. Schiefer, B. Draeger, J. Maier, and J. Ziegenhorn. 1985. Precipitation methods for the determination of LDL-cholesterol. *Clin. Biochem.* **18**: 118–125.
- Kraemer, M. P., S. Halder, S. S. Smyth, and A. J. Morris. 2018. Measurement of lysophosphatidic acid and sphingosine-1-phosphate by liquid chromatography-coupled electrospray ionization tandem mass spectrometry. *Methods Mol. Biol.* **1697**: 31–42.
- Hausmann, J., S. Kamtekar, E. Christodoulou, J. E. Day, T. Wu, Z. Fulkerson, H. M. Albers, L. A. van Meeteren, A. J. Houben, L. van Zeijl, et al. 2011. Structural basis of substrate discrimination and integrin binding by autotaxin. *Nat. Struct. Mol. Biol.* **18**: 198–204.
- Katsifa, A., E. Kaffe, N. Nikolaidou-Katsaridou, A. N. Economides, S. Newbigging, C. McKerlie, and V. Aidinis. 2015. The bulk of autotaxin activity is dispensable for adult mouse life. *PLoS One*. **10**: e0143083.
- Wang, J., L. Zhang, R. Xiao, Y. Li, S. Liao, Z. Zhang, W. Yang, and B. Liang. 2019. Plasma lipidomic signatures of spontaneous obese rhesus monkeys. *Lipids Health Dis.* **18**: 8.
- Weng, J., S. Jiang, L. Ding, Y. Xu, X. Zhu, and P. Jin. 2019. Autotaxin/lysophosphatidic acid signaling mediates obesity-related cardiomyopathy in mice and human subjects. *J. Cell. Mol. Med.* **23**: 1050–1058.
- Ackerman, S. J., G. Y. Park, J. W. Christman, S. Nyenhuis, E. Berdyshev, and V. Natarajan. 2016. Polyunsaturated lysophos-

- phatidic acid as a potential asthma biomarker. *Biomark. Med.* **10**: 123–135.
39. Zeng, R., B. Li, J. Huang, M. Zhong, L. Li, C. Duan, S. Zeng, J. Huang, W. Liu, J. Lu, et al. 2017. Lysophosphatidic acid is a biomarker for peritoneal carcinomatosis of gastric cancer and correlates with poor prognosis. *Genet. Test. Mol. Biomarkers.* **21**: 641–648.
  40. Kurano, M., A. Suzuki, A. Inoue, Y. Tokuhara, K. Kano, H. Matsumoto, K. Igarashi, R. Ohkawa, K. Nakamura, T. Dohi, et al. 2015. Possible involvement of minor lysophospholipids in the increase in plasma lysophosphatidic acid in acute coronary syndrome. *Arterioscler. Thromb. Vasc. Biol.* **35**: 463–470.
  41. Rother, E., R. Brandl, D. L. Baker, P. Goyal, H. Gebhard, G. Tigyi, and W. Siess. 2003. Subtype-selective antagonists of lysophosphatidic acid receptors inhibit platelet activation triggered by the lipid core of atherosclerotic plaques. *Circulation.* **108**: 741–747.
  42. Bot, M., I. Bot, R. Lopez-Vales, C. H. van de Lest, J. S. Saulnier-Blache, J. B. Helms, S. David, T. J. van Berkel, and E. A. Biessen. 2010. Atherosclerotic lesion progression changes lysophosphatidic acid homeostasis to favor its accumulation. *Am. J. Pathol.* **176**: 3073–3084.
  43. Chen, X., X. Y. Yang, N. D. Wang, C. Ding, Y. J. Yang, Z. J. You, Q. Su, and J. H. Chen. 2003. Serum lysophosphatidic acid concentrations measured by dot immunogold filtration assay in patients with acute myocardial infarction. *Scand. J. Clin. Lab. Invest.* **63**: 497–503.
  44. Siri-Tarino, P. W., S. Chiu, N. Bergeron, and R. M. Krauss. 2015. Saturated fats versus polyunsaturated fats versus carbohydrates for cardiovascular disease prevention and treatment. *Annu. Rev. Nutr.* **35**: 517–543.
  45. Rancoule, C., R. Dusaulcy, K. Treguer, S. Gres, C. Attane, and J. S. Saulnier-Blache. 2014. Involvement of autotaxin/lysophosphatidic acid signaling in obesity and impaired glucose homeostasis. *Biochimie.* **96**: 140–143.
  46. Nishimura, S., M. Nagasaki, S. Okudaira, J. Aoki, T. Ohmori, R. Ohkawa, K. Nakamura, K. Igarashi, H. Yamashita, K. Eto, et al. 2014. ENPP2 contributes to adipose tissue expansion and insulin resistance in diet-induced obesity. *Diabetes.* **63**: 4154–4164.
  47. Thumser, A. E., J. E. Voysey, and D. C. Wilton. 1994. The binding of lysophospholipids to rat liver fatty acid-binding protein and albumin. *Biochem. J.* **301**: 801–806.
  48. Tigyi, G., and R. Mileti. 1992. Lysophosphatidates bound to serum albumin activate membrane currents in *Xenopus* oocytes and neurite retraction in PC12 pheochromocytoma cells. *J. Biol. Chem.* **267**: 21360–21367.
  49. Jethwa, S. A., E. J. Leah, Q. Zhang, N. A. Bright, D. Oxley, M. D. Bootman, S. A. Rudge, and M. J. Wakelam. 2016. Exosomes bind to autotaxin and act as a physiological delivery mechanism to stimulate LPA receptor signalling in cells. *J. Cell Sci.* **129**: 3948–3957.
  50. Bouchareb, R., A. Mahmut, M. J. Nsaibia, M. C. Boulanger, A. Dahou, J. L. Lepine, M. H. Laflamme, F. Hadji, C. Couture, S. Trahan, et al. 2015. Autotaxin derived from lipoprotein(a) and valve interstitial cells promotes inflammation and mineralization of the aortic valve. *Circulation.* **132**: 677–690.
  51. Torzewski, M., A. Ravandi, C. Yeang, A. Edel, R. Bhindi, S. Kath, L. Twardowski, J. Schmid, X. Yang, U. F. W. Franke, et al. 2017. Lipoprotein(a) associated molecules are prominent components in plasma and valve leaflets in calcific aortic valve stenosis. *JACC Basic Transl. Sci.* **2**: 229–240.
  52. Chen, L., B. Liang, D. E. Froese, S. Liu, J. T. Wong, K. Tran, G. M. Hatch, D. Mymin, E. A. Kroeger, R. Y. Man, et al. 1997. Oxidative modification of low density lipoprotein in normal and hyperlipidemic patients: effect of lysophosphatidylcholine composition on vascular relaxation. *J. Lipid Res.* **38**: 546–553.
  53. Garnick, M. B., P. H. Bennett, and T. Langer. 1979. Low density lipoprotein metabolism and lipoprotein cholesterol content in southwestern American Indians. *J. Lipid Res.* **20**: 31–39.
  54. Blaho, V. A., S. Galvani, E. Engelbrecht, C. Liu, S. L. Swendeman, M. Kono, R. L. Proia, L. Steinman, M. H. Han, and T. Hla. 2015. HDL-bound sphingosine-1-phosphate restrains lymphopoiesis and neuroinflammation. *Nature.* **523**: 342–346.